Science of the Total Environment 878 (2023) 163171

Contents lists available at ScienceDirect

Science of the Total Environment

journal homepage: www.elsevier.com/locate/scitotenv

Dissolved organic matter defines microbial communities during initial soil formation after deglaciation

Jie Shen [a], Ziyan Liang [b], Yakov Kuzyakov [c,h], Weitao Li [d], Yuting He [e], Changquan Wang [f], Yang Xiao [a], Ke Chen [g], Geng Sun [a,*], Yanbao Lei [a,*]

[a] *China-Croatia "Belt and Road" Joint Laboratory on Biodiversity and Ecosystem Services, CAS Key Laboratory of Mountain Ecological Restoration and Bioresource Utilization & Ecological Restoration and Biodiversity Conservation Key Laboratory of Sichuan Province, Chengdu Institute of Biology, Chinese Academy of Sciences, Chengdu 610041, China*
[b] *Key Laboratory of Mountain Surface Processes and Ecological Regulation, Institute of Mountain Hazards and Environment, Chinese Academy of Sciences, Chengdu 610041, China*
[c] *Peoples Friendship University of Russia (RUDN University), 117198 Moscow, Russia*
[d] *CAS Key Laboratory of Tropical Forest Ecology, Xishuangbanna Tropical Botanical Garden, Chinese Academy of Sciences, Menglun, Mengla, Yunnan 666303, China*
[e] *Chengdu Popularization of Agricultural Technique Station, Chengdu 610041, China*
[f] *College of Resources, Sichuan Agricultural University, Chengdu 611130, China*
[g] *School of Life Science and Engineering, Southwest University of Science and Technology, Mianyang 621010, China*
[h] *Institute of Environmental Sciences, Kazan Federal University, 420049 Kazan, Russia*

HIGHLIGHTS

- DOM-microbial interactions were explored during post-glacial initial pedogenesis.
- DOM compounds in subsoil and at late stage were highly dehydrogenated and oxidized.
- Microbial succession shifted from copiotrophs to oligotrophs and saprophytes.
- Increased DOM-fungal negative networks promoted specialization of decomposition.
- Fungi decomposed stable DOM pools indicating increasing DOM persistence.

GRAPHICAL ABSTRACT

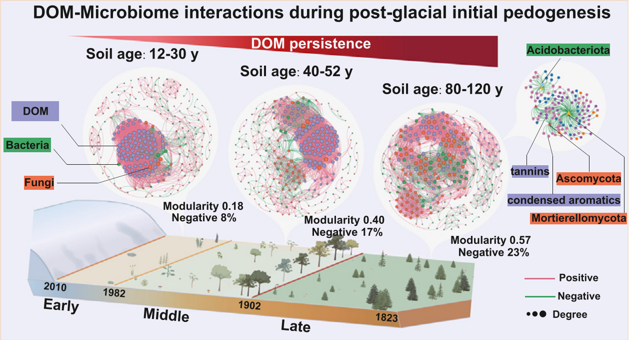

ARTICLE INFO

Editor: Jose Julio Ortega-Calvo

Keywords:
Dissolved organic matter
FT-ICR MS
Microbial community assembly
Glacier retreat
Initial soil formation
Ecosystem succession

ABSTRACT

Ecosystem succession and pedogenesis reshuffle the composition and turnover of dissolved organic matter (DOM) and its interactions with soil microbiome. The changes of these connections are especially intensive during initial pedogenesis, e.g. in young post-glacial areas. The temporal succession and vertical development of DOM effects on microbial community structure remains elusive. Using Fourier Transform Ion Cyclotron Resonance Mass Spectrometry (FT-ICR MS), high-throughput sequencing, and molecular ecological networks, we characterized the molecular diversity of water-extractable DOM and identified its links to microbial communities in soil profiles along deglaciation chronosequence (12, 30, 40, 52, 80, and 120 years) in the southeastern Tibetan Plateau. Low-molecular-weight compound content decreased, whereas the mid- and high-molecular-weight compounds increased with succession age and soil depth. This was confirmed by the increase in double bond equivalents and averaged oxygen-to-carbon ratios (O/C), and decrease in hydrogen-to-carbon ratios (H/C), which reflect DOM accumulation and stabilization. Microbial community succession shifted towards the dominance of oligotrophic *Acidobacteria* and saprophytic *Mortierellomycota*, reflecting the increase of stable DOM components ($H/C < 1.5$ and wider O/C). Less DOM-bacterial positive networks during the succession reduced specialization of labile DOM production (such as lipid- and protein-like compounds), whereas more DOM-fungal negative networks increased specialization of stable DOM decomposition (such as

---

* Corresponding authors at: Chengdu Institute of Biology, Chinese Academy of Sciences, Number 9, Renmin South Road, Wuhou District, Chengdu City, Sichuan Province 610041, China.
E-mail addresses: sungeng@cib.ac.cn (G. Sun), leiyb@cib.ac.cn (Y. Lei).

http://dx.doi.org/10.1016/j.scitotenv.2023.163171
Received 14 January 2023; Received in revised form 22 March 2023; Accepted 26 March 2023

tannin- and condensed aromatic-like compounds). Consequently, DOM stability is not intrinsic during initial pedogenesis: stable DOM compounds remain after fast bacterial utilization of labile DOM compounds, whereas fungi decompose slowly the remaining DOM pools.

1. Introduction

Increasing concerns about global warming have drawn attention to the role of dissolved organic matter (DOM) in the cycling and redistribution of ecosystem carbon (C) and nutrients (Hu et al., 2022). As the most mobile and bioavailable constituent of soil organic matter (Vujinović et al., 2020), DOM heterogeneity is intimately linked to microbial activities (Tian et al., 2012; Zhang et al., 2018). Microbial communities are the driving force of DOM formation, consumption, and transformation, especially in pristine and young ecosystems, such as glacier retreat areas (Castle et al., 2017; Jiang et al., 2019). Glacier retreat-driven vegetation succession and the parallel ongoing pedogenesis increases the diversity of organic substances and soil microbiome (Bradley et al., 2016; Jiang et al., 2018; Gyeong et al., 2021). A high microbial diversity provides more metabolic pathways to continuously recycle, transform, and assemble DOM molecules, which influences the molecular weight, chemical structure, oxidation state, and bioavailability of DOM (Kaiser and Kalbitz, 2012; Zark and Dittmar, 2018; Roth et al., 2019). However, the routes of DOM formation and microbial community succession are usually studied independently (Wu et al., 2018), despite DOM is the main source of C and energy for soil microorganisms (Tian et al., 2012). The magnitude and directions of DOM-microbial interactions have not yet been quantified on the deglaciated area, which are fundamental to evaluate DOM fate and persistence during initial soil formation.

The mechanisms involved in deglaciation-derived DOM-microbial interactions may be attributed to two proximal drivers. First, vegetation succession influences DOM composition and bio-availability. Plant supplies leaf litter, rhizodeposits including root exudates, and decaying fine roots, all of which are DOM sources and are crucial for microbial metabolism (Franklin et al., 2020). Plant residue components can be ranked as soluble compounds, hemicellulose, cellulose, lipids, and lignin by fastest to slowest degradability (Shipley and Tardif, 2020; Wang et al., 2022). Second, soils on the deglaciated area undergo a progressive profile development, which alters microbial habitats, decreases soil pH and increases organic matter content, cation exchange capacity, porous structure and accelerate mineral weathering (He and Tang, 2008). Although an increase in clay minerals favors the sorption of organic substances (Saidy et al., 2013), microbial processing may remobilize mineral-bound DOM molecules (Kaiser and Kalbitz, 2012). For instance, plant-derived polymers are hydrolyzed and oxidized stepwise from soluble compounds to lignin and microbially transformed into microbially-derived compounds (Waggoner et al., 2015). Thus, soil microbiome affects the DOM composition and content and is at the same time dependent of them (Wen et al., 2022). The succession of DOM molecular diversity and the linked microbial networks remain largely unexplored, whereas the recently deglaciated areas provide ideal objects for such studies, because of the low interaction complexity during initial soil formation.

Soil microorganisms modify the chemical structure and molecular weight of DOM by utilization and decomposition (Sanderman et al., 2008; Wen et al., 2022). Hu et al. (2022) constructed the molecular ecological networks (MENs) to quantify DOM-microbial interactions: i) negative MENs correlations indicate the DOM decomposition; ii) positive MENs correlations indicate DOM production via biosynthesis. Such assemblages of DOM-microbial MENs depend on microbial life-history traits (Fierer et al., 2007; Muscarella et al., 2019). The *r*-selected copiotrophs (resource generalists, growth and resource acquisition strategy) focus on consuming labile DOM, whereas *K*-selected oligotrophs (resource specialists, compete and survive strategy) mediate slow DOM turnover (Fierer et al., 2007; Roth et al., 2019). In natural ecosystems, continuous litter inputs form stable C pools due to the increasing dominance of fungi (resource specialists) rather than bacteria (resource generalists) (Wei et al., 2022). Although vegetation succession from nitrogen (N_2)-fixing shrubs to broadleaved and coniferous trees is accompanied by conversion of nutrient-rich to nutrient-poor substrates on recently deglaciated areas (Jiang et al., 2018; Jiang et al., 2019; Lei et al., 2021), challenges remain regarding nutrient limitation effects on the DOM persistence via resource generalists or specialists.

Soil DOM consists of a highly complex and heterogeneous molecular compounds, and only a few DOM molecules (no >5 %) have been definitively classified to date (Zark and Dittmar, 2018). Previous progress in DOM analytical techniques, such as excitation-emission matrix (EEM) (Zeng et al., 2017), Fourier transform infrared (FTIR) spectroscopy (Minor et al., 2014), nuclear magnetic resonance (NMR) spectroscopy (Neilen et al., 2019), and pyrolysis gas chromatography–mass spectrometry (Py-GC–MS) (Kallenbach et al., 2016; Leinweber et al., 2008), have provided comprehensive insights into DOM chemo-diversity. However, these approaches provide limited types of DOM compounds and functional groups, because DOM is primarily regarded as a whole for analysis (Li et al., 2019).

Recent advances in Fourier transform ion cyclotron resonance mass spectrometry (FT-ICR MS) have expedited the parsing of in-depth DOM components (Zark et al., 2017; Zark and Dittmar, 2018). FT-ICR MS enables the complete separation and analysis of complex mass peaks and their counterpart molecular formula within DOM pools owing to its ultra-high resolution (>200,000) and accuracy (error < 1 ppm) (He et al., 2018; Hu et al., 2022). Currently, the integration of FT-ICR MS and high-throughput sequencing enables detailed characterization of DOM-microbial associations in marine (Osterholz et al., 2016; Zark et al., 2017), lake (Tanentzap et al., 2019), and soil ecosystems (Li et al., 2018a, 2018b), whereas DOM characterization in soils of deglaciated areas is still in its infancy (Broadbent et al., 2021; Wu et al., 2021).

The Hailuogou deglaciated chronosequence in the southeastern Tibetan Plateau comprises a 120-year primary vegetation succession and pedogenesis, which has undergone a progressive transition from the pioneer moss to the climax forest stage (Lei et al., 2015; Lei et al., 2021). Previous studies have focused on primary succession in soil development (Zhou et al., 2013), microbial processes, and nutrient limitations (Jiang et al., 2018; Jiang et al., 2019; Zhou et al., 2019; Lei et al., 2021). Here, the fundamental knowledge regarding temporal succession in labile/stable DOM components and its interactions with microbial assemblages (for example, *r*-selected copiotrophs vs. *K*-selected oligotrophs or resource generalists vs. resource specialists) is critical to understand C dynamics. By integrating FT-ICR MS, high-throughput sequencing, and MENs approaches, we characterized the effects of primary succession on DOM-microbial interactions along the glacier foreland chronosequence (12, 30, 40, 52, 80, and 120 years), to address the following questions: i) *at a structural level*: how does DOM molecular composition change during initial soil development and with depth? ii) *at a molecular network level*: how does microbial communities interact with DOM components during initial soil formation?

2. Materials and methods

2.1. Study area and sampling design

The study area is located in Hailuogou Glacier Chronosequence area (29°34′07.83″ N, 101°59′40.74″ E) that lies on Gongga Mountain (7556 m above sea level), Southeastern Tibetan Plateau (Fig. S1). This area has a mean annual temperature of 3.8 °C (ranging from −4.3 °C to 12.7 °C), mean annual precipitation is 1947 mm, and the elevation ranges from 2800 m to 3400 m above sea level. A gradual recession of Hailuogou glacier is observed since 1823, with an acceleration from the early 20th century, which developed from the terminal moraine and reached the northeast about 2 km (Fig. S1), and has undergone a progressive vegetation succession from pioneer moss stage to climax forest stage (Table S1) (Lei et al., 2015; Zhou et al., 2018; Lei et al., 2021). At this deglaciated area, previous studies have investigated soil development (He and Tang, 2008), nutrient cycling (Zhou et al., 2013; Zhou et al., 2018; Jiang et al., 2019; Zhou et al., 2019) and microbial changes (Jiang et al., 2018; Li et al., 2023).

In August 2020, a total of 36 soil samples were collected (six succession ages × two soil depths × three replicates). Six sites representing succession ages (12, 30, 40, 52, 80 and 120 years since glacier retreat). Two soil depths (topsoil: 0–10 cm; subsoil: 10–20 cm) and three replicates (5 × 5 m square with >10 m apart) were sampled for each succession age. To avoid block effects among three replicates and obtain representative and reproducible soil samples, we used a nested five-point sampling strategy at each replicate (Baker et al., 2009): five soil cores from the same depth were mixed to form a composite sample. After removing the roots, litter, and stones, soil samples were sieved through a 2 mm mesh for homogeneity (Mushinski et al., 2018). After sampling, soil samples were immediately transported to the laboratory in aseptic-refrigeration boxes. For each sample, approximately 500 g soil was partitioned into two parts: one section was stored at 4 °C for soil chemical analysis, the other was stored at −80 °C for solid-phase extraction of DOM (SPE-DOM) and DNA extraction.

2.2. Chemical characterization and DOM analysis

Soil (8 g) was weighed and placed into tubes, and 40 mL ultrapure water (1:5 soil: water ratio) was added. The tubes were shaken (170 rpm) for 8 h and were centrifuged at 4000 ×g for 10 min (25 °C). The supernatant was collected and filtrated through a 0.45 μm filter membrane and stored at 4 °C, then the content of dissolved organic C and dissolved organic N were analyzed using a total organic carbon (TOC) analyzer (Liquic TOC, Elementar, Germany) (Huang et al., 2012).

Solid-phase extraction of DOM (SPE-DOM) from the soil was performed according to the procedure as previously described (Li et al., 2019). First, the DOM was extracted from the soil samples (40 g) using 200 mL ultrapure water (1:5 soil: water ratio) on a reciprocal shaker (170 rpm) for 8 h. Samples were then centrifuged at 4000 ×g for 10 min, and an equal amount of supernatant was extracted from each sample (180 mL) to filter (0.45 μm) and store at 4 °C. SPE cartridges (500 mg, Agilent Technologies, Santa Clara, CA) were activated by methanol (20 mL), and were rinsed with acidified ultrapure water (20 mL, pH = 2.0). After that, the DOM was loaded on the SPE cartridges via gravity. The SPE cartridges were dried by ultrapure N_2, then DOM were eluted with methanol (5 mL) and stored at −20 °C. The molecular components of SPE-DOM were analyzed using a 15 T SolariX FT-ICR mass spectrometer (FTMS, Bruker Daltonics) operating in negative mode. Samples were continuously injected into the ESI source (200 μL volume per injection) with a flow rate of 120 $\mu L\ h^{-1}$ and a molecular-weight range of 100–1600 Da (Blackburn et al., 2017), and 300 single scans with an ion accumulation time of 0.06 s were conducted (Roth et al., 2019). The instrument was calibrated with sodium formate (10 mmol/L). After calibration, the mass error of all compounds was <1 ppm. To determine possible contamination, blanks and solvent blanks were collected during the extraction process, and the following data processing did not consider the mass peaks with S/N less than six (Lucas et al., 2016; Li et al., 2018a, 2018b).

Using Data Analysis 4.4 (Bruker Daltonics), the raw spectra were converted to a list of *m/z* values based on FTMS peak picker. Molecular formulas with C, H, O, S element were assigned using Formularity software. Individual molecular formulas were cross-plotted in a van Krevelen diagram based on their elemental ratios of oxygen-to-carbon (O/C, x-axis) and hydrogen-to-carbon (H/C, y-axis). All assigned formulas must meet the criteria: (1) mass accuracy < 0.5 ppm; (2) only formulas of $0.3 < H/C < 2.2$ with $O/C < 1.2$ were retained (Wang et al., 2016). Then, the formulas in the van Krevelen diagram were assigned into eight groups (Li et al., 2018a, 2018b): (1) lipid-like compounds (O/C: 0–0.3, H/C: 1.5–2.0), (2) protein/amino sugar-like compounds (O/C: 0.3–0.67, H/C: 1.5–2.2), (3) carbohydrate-like compounds (O/C: 0.67–1.2, H/C: 1.5–2.4), (4) unsaturated hydrocarbon compounds (O/C: 0–0.1, H/C: 0.7–1), (5) lignin-like compounds (O/C: 0.1–0.67, H/C: 0.7–1.5, AI < 0.67), (6) tannin-like compounds (O/C: 0.67–1.2, H/C: 0.5–1.5, AI < 0.67), (7) condensed aromatic-like compounds (O/C: 0–0.67, H/C: 0.2–0.7, AI ≥ 0.67), (8) others (compounds that were not part of the above seven groups).

2.3. 16S rRNA gene sequencing and microbial community analysis

Following the manufacturer's instructions, the total DNA from soil (0.5 g) was extracted using FastDNA® SPIN Kit by MP Biomedicals, USA. Using NanoDrop 2000 spectrophotometer (Thermo Scientific, USA) and 1 % agarose gel electrophoresis to measure and assess the DNA quantity and quality. Total DNA was stored at −80 °C until sequencing.

Using a thermocycler PCR system (GeneAmp 9700, USA), V3-V4 hypervariable regions of bacterial 16S rRNA gene was amplified with primers 515F (5′-GTGCCAGCMGCCGCGG-3′) and 907R (5′-CCGTCAATTCMTTTRAGTTT-3′) (Jiang et al., 2018). Fungal ITS rRNA gene is targeted by primers ITS1F (5′-ACTTGGTCATTTAGAG-GAAGTAA-3′) and ITS2R (5′-BGCTGCGTTCTTCATCGATGC-3′) (Shen et al., 2022). The purified and mixed PCR products were then sequenced (Illumina MiSeq platform, USA) by Majorbio, Inc. (Shanghai, China). Raw sequences were filtered and merged using QIIME 1.9.1 and FLASH 1.2.11, respectively. Operational taxonomic units (OTUs) were defined using a 97 % similarity. All sequencing files are publicly available through the NCBI Sequence Read Archive (SRA) database with BioProject ID: PRJNA880367.

2.4. Statistical analysis

The effects of succession age, soil depth, and their interactions on soil DOM contents were tested with two-way ANOVA, with post-hoc comparisons using Tukey's HSD (honest significant difference) method in SPSS 25.0. Absolute FT-ICR-MS signal intensities of assigned molecular formula were used to characterize DOM molecular-weight spectra (*m/z* range 100–800 Da). The low-molecular-weight ($m/z = 100–300$ Da), mid-molecular-weight ($m/z = 300–450$ Da), and high-molecular-weight ($m/z = 450–800$ Da) range was defined by Roth et al. (2019). Aromaticity index (AI), double bond equivalent (DBE), molecular weight (MW), hydrogen-to-carbon ratio (H/C), and oxygen-to-carbon ratio (O/C) were calculated according to the elemental composition of molecular formula (Koch and Dittmar, 2006; Li et al., 2019):

$$AI = \frac{1 + \mathrm{C} - 0.5\mathrm{O} - \mathrm{S} - 0.5\mathrm{H}}{C - 0.5O - S - N}$$

$$\mathrm{DBE} = 1 + \frac{2C - H + N}{2}$$

Furthermore, weighted averages of DBE_w, MW_w, H/C_w and O/C_w were calculated as follows: $DBE_w = sum((DBE_i \times I_i)/\Sigma(I_i))$; $MW_w = sum((MW_i \times I_i)/\Sigma(I_i))$; $H/C_w = sum((H/C_i \times I_i)/\Sigma(I_i))$; $O/C_w = sum((O/C_i \times I_i)/\Sigma(I_i))$, in which DBE_i, MW_i, H/C_i and O/C_i were individual information and I_i was signal intensity (Roth et al., 2019).

Venn analysis (http://bioinformatics.psb.ugent.be/webtools/Venn/) was performed to characterize the numbers and percent of molecular formulas unique to each soil age or depth (unique group) and shared by different soil ages or depths (sharing group). The sum of unique and sharing group was the numbers and percent of molecular formulas (abundant group) in each soil age or depth. Polynomial regressions between succession age and DOM molecular stoichiometry were performed using Origin 2022. Nonmetric multidimensional scaling (NMDS) was used to assess the compositional similarity in DOM molecular formulas and microbial community using "vegan" package in R version 4.1.2 (Peng et al., 2018). Linear discriminant analysis (LDA) effect size (LEfSe) was performed online (http://huttenhower.sph.harvard.edu/lefse/) with the logarithmic LDA score threshold set to 2.0 (Segata et al., 2011), to intensify DOM chemo-markers among succession ages and soil depths. The "psych" package in R version 4.1.2 was used to compute Pearson product-moment correlations between DOM molecular formulas and microbial OTUs ($r > |0.9|$, $p < 0.05$) (Lucas et al., 2016). The DOM-microbial associations were visualized using Cytoscape (3.9.1) (Lucas et al., 2016) and Gephi (0.9.2) (Li et al., 2019). Other graphical work was accomplished using Origin 2022, R package ggplot2, and Adobe Illustrator 2021.

3. Results

3.1. DOM molecular characteristics along the chronosequence

Over the 120-year chronosequence of the glacier retreat, soil DOM content increased with succession age ($p < 0.001$, Table 1), with the largest increase at 80- and 120-years. DOM content also changed with soil depth, especially in dissolved organic C ($p < 0.05$, Table 1). The interactions between soil age and depth on dissolved organic C were significant ($p < 0.001$, Table 1).

Using FT-ICR-MS, 42,950 unique DOM molecular formulas were identified. Compared with the low-molecular-weight range (m/z = 100–300 Da), the absolute intensity of mid- (m/z = 300–450 Da) and high-molecular-weight (m/z = 450–800 Da) increased with succession age, and was higher in the subsoil than in the topsoil (Fig. 1a). During soil development, MW, DBE, and O/C ratio increased ($p < 0.001$), whereas the H/C ratios decreased ($p < 0.001$) (Fig. 1b).

There were significant DOM differences among succession ages (Stress = 0.07) (Fig. 2a). Based on NMDS distances of molecular DOM structure, we defined three stages of glacier retreat: early (12- and 30-year), middle (40- and 52-year), and late stage (80- and 120-year). The total number of abundant molecular formulas decreased from the early to late stage (Fig. 2b). The percentage of unique molecular formulas in the early (32 %), middle (21 %), and late stage (17 %) were 2.3-, 1.5-, and 1.2-fold larger than those in the sharing group (14 %) (Fig. 2b), and the molecular formulas unique to the topsoil (37 %) and subsoil (35 %) were 1.4- and 1.3-fold higher than their sharing group (27 %), respectively (Fig. 2c).

Table 1
Content of dissolved organic C and N averaged over succession age (SA) and soil depth (SD).

Succession age	Dissolved organic C mg kg^{-1} soil (s.e.)	Dissolved organic N mg kg^{-1} soil (s.e.)
Topsoil		
12-year	18.5 (1.5) cB	4.9 (0.9) b
30-year	19.7 (5.2) cB	9.2 (2.7) b
40-year	80.3 (10.1) b	28.4 (3.1) bA
52-year	118.0 (13.0) bA	47.9 (20.7) b
80-year	478.2 (24.8) a	98.5 (26.4) a
120-year	476.9 (14.1) aB	127.9 (28.2) a
Subsoil		
12-year	54.7 (3.8) cA	3.3 (0.7) b
30-year	68.1 (15.8) cA	5.8 (2.8) b
40-year	81.7 (23.2) c	15.6 (3.0) bB
52-year	58.1 (15.9) cB	11.9 (4.2) b
80-year	492.0 (25.5) b	51.6 (40.0) ab
120-year	973.2 (54.8) aA	129.8 (52.8) a
F-Radio		
SA	340.0***	8.6***
SD	48.1***	1.5
SA × SD	41.3***	0.4

Values: means (SE), n = 3; a, b, c Significant differences among retreating age; A, B Significant differences between topsoil and subsoil.
*** $p < 0.001$.

3.2. Chemo-diversity and chemo-markers of DOM molecular formulas depending on soil age

The van Krevelen diagram (O/C ratio vs. H/C ratio) of the DOM compounds (Fig. 2d, e) clearly showed that lipid- and protein-like compounds (H/C ≥ 1.5), and unsaturated hydrocarbon compounds (O/C = 0.1, H/C = 0.7–1) decreased with succession age and soil depth. Unique DOM molecular formulas in the late stage and subsoil were dominated by tannin-like compounds with O/C = 0.67–1.2 and H/C = 0.5–1.5.

Relative proportion of the DOM components differed significantly among soil ages (ANOSIM, $R = 0.46$, $p = 0.001$) and between soil depths (ANOSIM, $R = 0.40$, $p = 0.01$) (Fig. 3a). The proportions of carbohydrate-, protein-, and lipid-like compounds declined with soil age and depth, whereas tannin- and condensed aromatic-like compounds were strongly enriched with soil age and depth (Fig. 3a). The lignin-like compounds were considerably enriched during the middle stage (Fig. 3a).

Using LEfSe analysis, a total of 674 and 48 DOM molecular formulas (referred as chemo-markers) were identified to explain the greatest difference among succession stages. These chemo-markers were then plotted in van Krevelen diagram (O/C ratio vs. H/C ratio) to simplify the analysis of the major groupings (Fig. 3b, c). The DOM chemo-markers in the early stage and topsoil were dominated by lipid- and protein-like compounds belonging to labile organic compounds (H/C ≥ 1.5, O/C < 0.67). Conversely, chemo-markers in the late stage and subsoil were indicative for persistent compounds with wider O/C and H/C < 1.5, that is, tannin- and condensed aromatic-like compounds. The chemo-markers in the middle stage were the lignin-like compounds (H/C = 0.7–1.5 and O/C = 0.1–0.67).

3.3. Microbial community shift during initial soil development

NMDS analysis revealed that the succession stages clearly determined the microbial community assemblage (stress: bacteria = 0.06; fungi = 0.11) (Fig. 4a, b). The dominant bacteria across all soils were *Proteobacteria* (33–43 %, Fig. 4c). Other prevalent bacteria were *Acidobacteria*, *Actinobacteria*, and *Bacteroidota* (>8 %) (Fig. 4c). The relative abundance of *Acidobacteria* increased during succession (ANOVA, $p < 0.001$), whereas *Actinobacteriota* ($p < 0.01$) and *Chloroflexi* ($p < 0.01$) decreased. *Methylomirabilota* ($p < 0.01$) and *Gemmatimonadota* ($p < 0.01$) increased until 52-year, and then decreased.

Ascomycota dominated the fungal communities in all soils (13–63 %), and *Basidiomycota*, *Rozellomycota*, and *Mortierellomycota* were additional prevalent phyla (>10 %) (Fig. 4d). The relative abundance of *Rozellomycota* ($p < 0.01$) decreased with increasing soil age, whereas *Basidiomycota* ($p < 0.001$) and *Mortierellomycota* ($p < 0.001$) increased. The abundance of *Ascomycota* ($p < 0.05$) in the middle stage was higher than in the early and late stages.

3.4. Molecular ecological networks (MENs) of DOM and microorganisms during initial soil development

A co-occurrence network analysis (3-stage × 2-depth series MENs) allowed to quantify the DOM-microbial interactions and provided a molecular-level perspective regarding the associations between specific DOM molecular formulas and microbial taxa. There were strong interactions between DOM molecular formulas and bacterial and fungal communities, whereas the succession trajectories of MENs were dependent on the soil age and depth (Fig. 5).

According to the resource-consumer relationships of DOM-microbial MENs, positive interactions indicate the production of new molecules via biosynthetic processes, whereas negative interactions relate to the decomposition of larger molecules to smaller molecules. Compared to the early stage, the proportion of positive edges declined in middle and late MENs (23 % and 13 %, respectively). In contrast, the negative edges increased from 8 % (early stage) to 31 % (middle stage) and 22 % (late stage) (Fig. 5a). Based on degree and closeness centrality, 68 (DOM: 66, bacteria: 1, fungi: 1) network hubs were detected in the early stage, and only 48

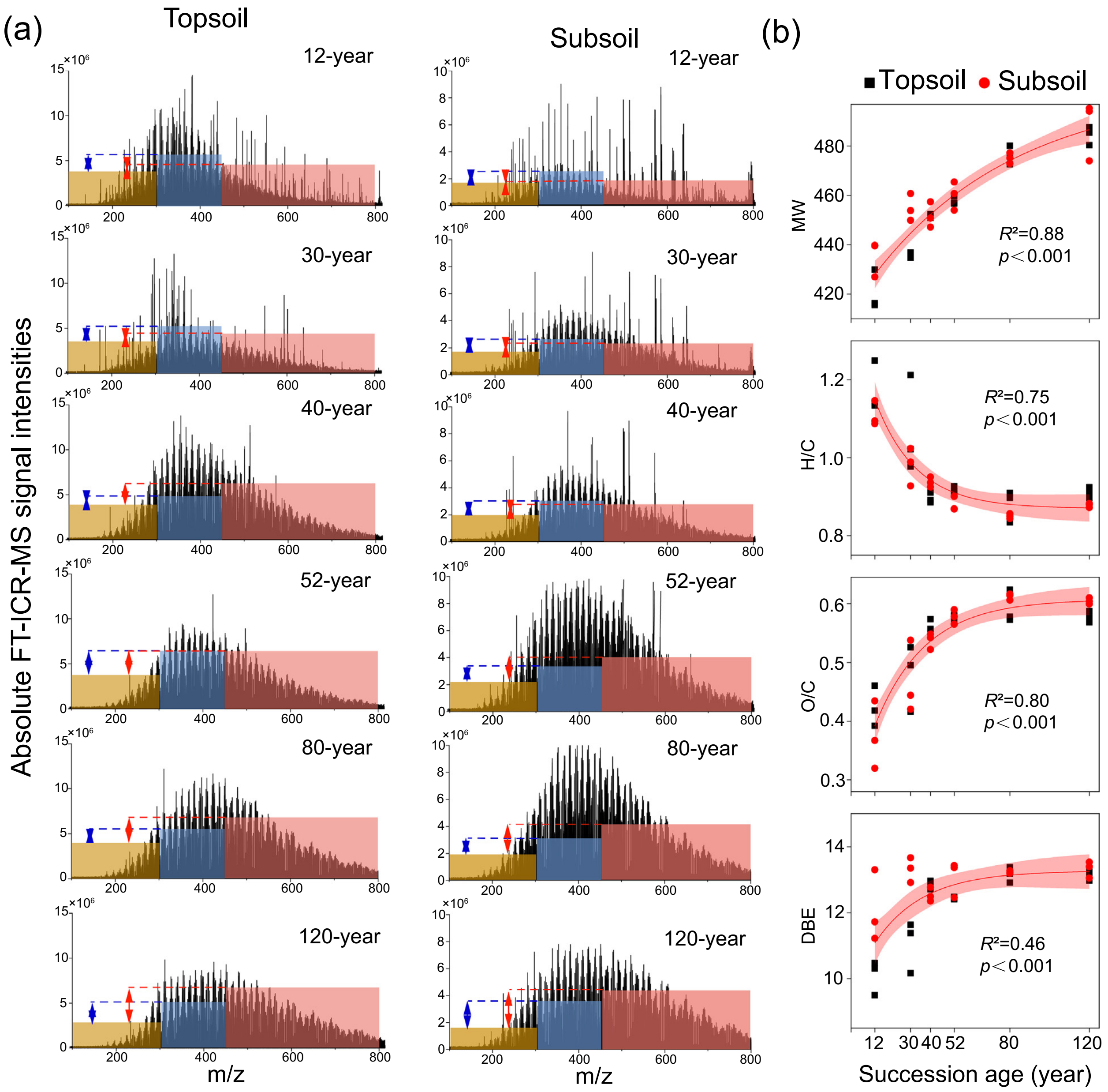

Fig. 1. Molecular changes of DOM based on FT-ICR mass spectra. (a) DOM molecular-weight spectra (absolute FT-ICR-MS intensities of all detected signals) in each soil age and soil depth (mean spectrum of all replicates was included in data presentation). The intensity (75 % quartile) for the low-molecular-weight range (mass-to-charge ratio m/z = 100–300 Da) is highlighted yellow, for the mid-molecular-weight range (m/z = 300–450 Da) it is highlighted blue, and for the high-molecular-weight range (m/z = 450–800 Da) it is highlighted red. (b) Magnitude-weighted parameters of DOM compounds during ecosystem succession (exponential regressions). MW, intensity weighted molecular weight; H/C, intensity weighted averaged hydrogen to carbon ratios of assigned molecular formulas; O/C, intensity weighted averaged oxygen to carbon ratios of assigned molecular formulas; DBE, intensity weighted averaged double bond equivalent.

(DOM: 41, bacteria: 3, fungi: 4) network hubs were detected in the late stage, whereas none were found in the middle stage. The negative DOM-fungi edges increased during the glacier retreat stage (slope = 2.52; R^2 = 0.94) (Fig. S2).

Compared to the topsoil, the changes were more pronounced at the edges of subsoil MENs, in which the proportion of positive edges strongly decreased during succession (92 % to 77 %), while negative edges increased (from 8 % to 23 %). Network hubs of DOM decreased (84 to 67) with soil age, whereas hubs of microbes strongly increased (bacteria, 1.6- and 4.5-fold increases; fungi, 0.5- and 4.8-fold increases). The negative DOM-bacteria edges increased during the glacier retreat stage (slope = 2.52; R^2 = 0.99) (Fig. S2).

The temporal succession of network topological parameters in the subsoil was more pronounced than in the topsoil (Table S2). Edge numbers decreased with soil age, as did the average clustering coefficient and graph density. In contrast, modularity of DOM-microbial MENs substantially increased (0.18 to 0.57) during the succession.

4. Discussion

Primary succession of vegetation and soils on the deglaciated area defines molecular DOM-microbial networks during a 120-year pedogenesis. We elucidated that the temporal succession and vertical soil development define DOM molecular weight, stoichiometry, composition, oxidation

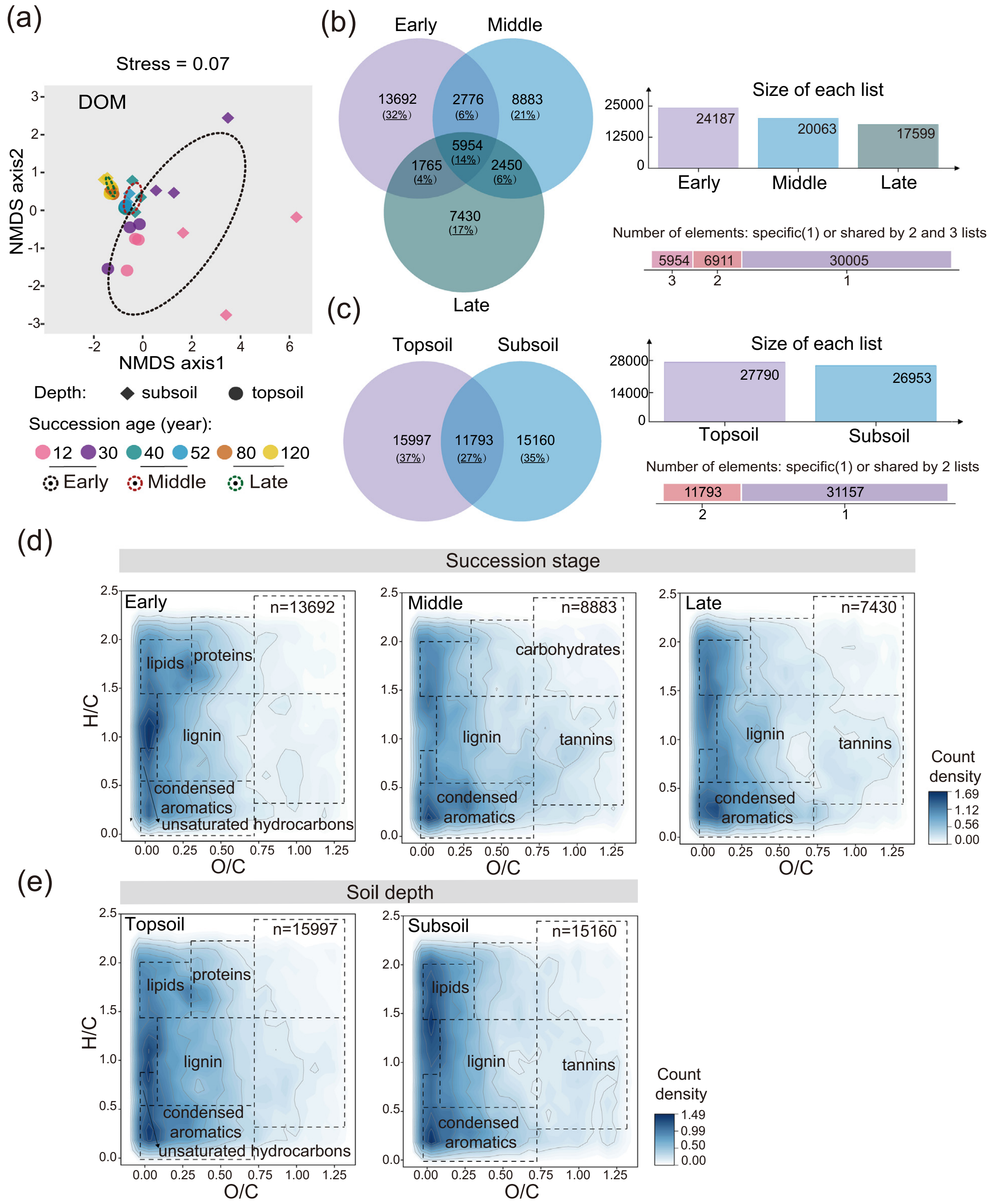

Fig. 2. Distribution patterns of DOM molecular composition depending on succession stages and soil depth. (a) Nonmetric multidimensional scaling (NMDS) ordinations of DOM molecular formulas based on Bray-Curtis distance. (b)–(c) Venn diagrams showing the number and percent (%) of the abundant molecular formulas. (d)–(e) van Krevelen diagram-derived distribution patterns of unique DOM components in each succession stage and soil depth based on the O/C and H/C ratios. Count density indicates the occurrence frequency of molecular formulas in the area of diagrams.

state and so, reshape the microbial community. The structural shift in DOM-microbial networks through succession age and soil depth with increasing connectivity and modularity of DOM-fungal negative networks reflect the increased fungal specialization to decompose stable DOM pools and raised DOM persistence.

4.1. DOM composition during pedogenesis

DOM interactions with microorganisms depend on the molecular traits of DOM, such as its bioavailability, measured by molecular weight, hydrogen to carbon ratios, oxygen to carbon ratios, and averaged double bond

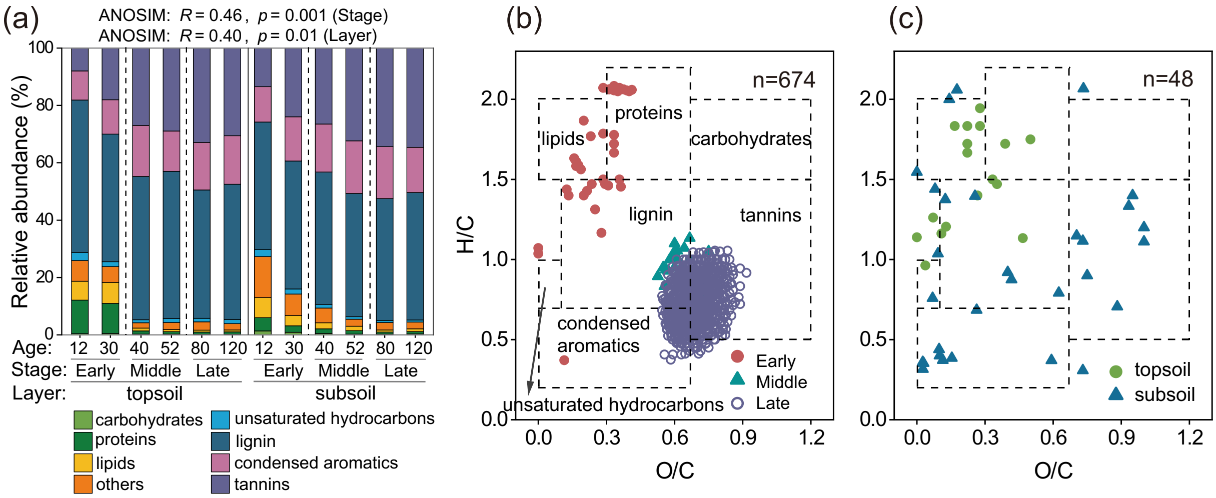

Fig. 3. Chemo-diversity and chemo-marker of DOM molecular formulas. (a) Relative proportion of the DOM components. Relative proportion of each molecular formula was calculated using spectra intensity of each formula divided by the sum of all intensities. (b) Linear discriminant effect size analysis (LEfSe) of DOM chemo-markers that are enriched depending on succession stages and soil depths.

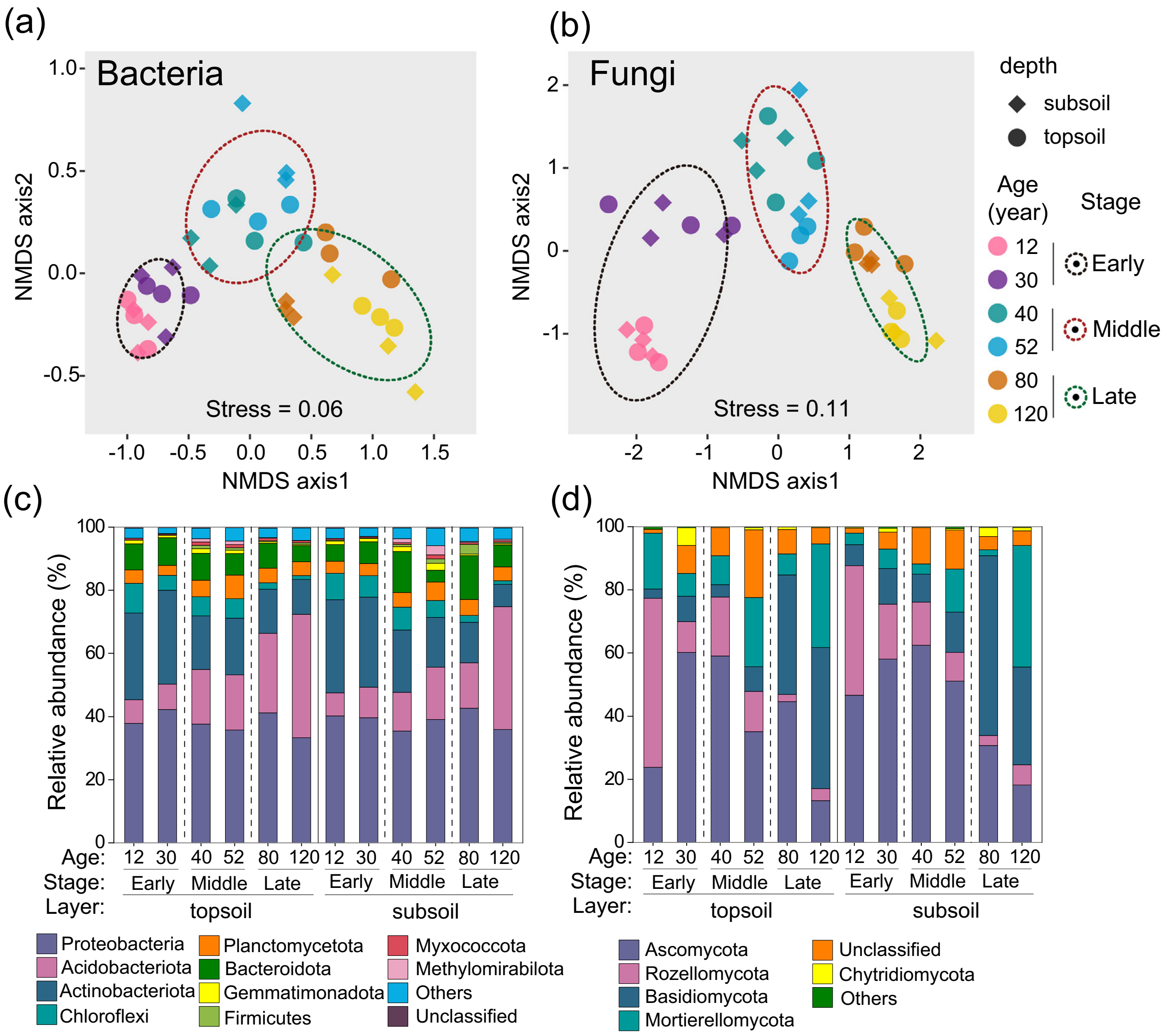

Fig. 4. Characterization of microbial community composition. NMDS ordinations of bacterial (a) and fungal (b) communities based on Bray-Curtis distance. Relative abundance of bacterial (c) and fungal (d) community compositions at the phylum level.

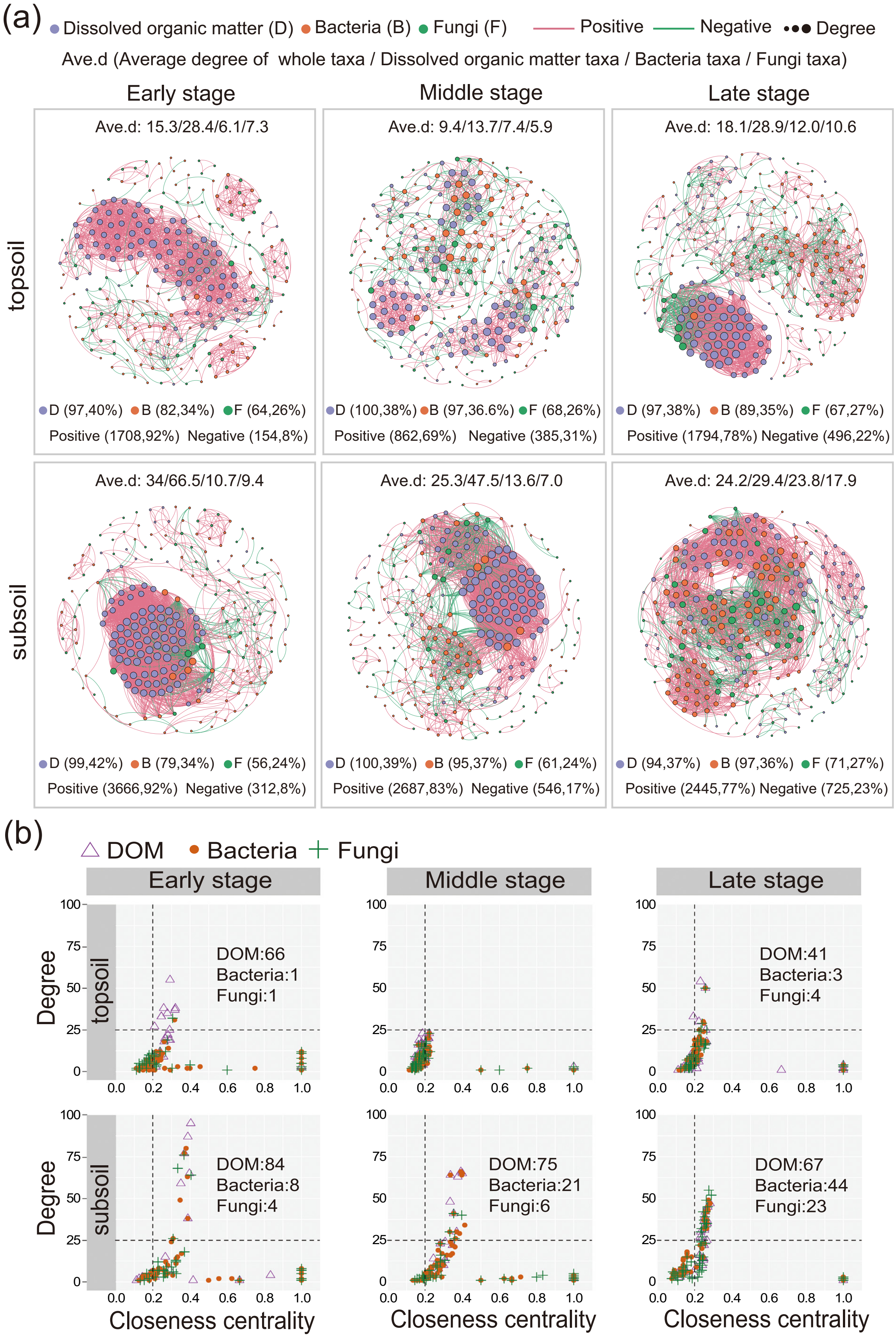
(a)
Dissolved organic matter (D) Bacteria (B) Fungi (F) Positive Negative Degree
Ave.d (Average degree of whole taxa / Dissolved organic matter taxa / Bacteria taxa / Fungi taxa)
Early stage
Middle stage
Late stage
topsoil
Ave.d: 15.3/28.4/6.1/7.3
D (97,40%) B (82,34%) F (64,26%)
Positive (1708,92%) Negative (154,8%)
Ave.d: 9.4/13.7/7.4/5.9
D (100,38%) B (97,36.6%) F (68,26%)
Positive (862,69%) Negative (385,31%)
Ave.d: 18.1/28.9/12.0/10.6
D (97,38%) B (89,35%) F (67,27%)
Positive (1794,78%) Negative (496,22%)
subsoil
Ave.d: 34/66.5/10.7/9.4
D (99,42%) B (79,34%) F (56,24%)
Positive (3666,92%) Negative (312,8%)
Ave.d: 25.3/47.5/13.6/7.0
D (100,39%) B (95,37%) F (61,24%)
Positive (2687,83%) Negative (546,17%)
Ave.d: 24.2/29.4/23.8/17.9
D (94,37%) B (97,36%) F (71,27%)
Positive (2445,77%) Negative (725,23%)
(b)
DOM Bacteria Fungi
Early stage
Middle stage
Late stage
Degree
topsoil
subsoil
0
25
50
75
100
0.0
0.2
0.4
0.6
0.8
1.0
DOM:66
Bacteria:1
Fungi:1
DOM:41
Bacteria:3
Fungi:4
DOM:84
Bacteria:8
Fungi:4
DOM:75
Bacteria:21
Fungi:6
DOM:67
Bacteria:44
Fungi:23
Closeness centrality

equivalent (D'Andrilli et al., 2015). Based on molecular formulas obtained from FT-ICR-MS, low-weight DOM (m/z = 100–300) decreased, but mid- and high-weight DOM ($m/z > 300$) increased with soil age after glacier retreat. These effects were more pronounced in the subsoil than in the topsoil (Fig. 1a). This change is typically followed by a substantial increase in unsaturated molecules (Roth et al., 2019), as indicated by the MW, DBE, and O/C ratio increased and H/C ratio decreased during pedogenesis (Fig. 1b). Consequently, the dehydrogenated and oxygen-enriched components dominate the DOM with increasing soil age (Šantl-Temkiv et al., 2013; Osterholz et al., 2016). Chemo-markers (van Krevelen diagram and LEfSe-derived differential mass spectra, Fig. 3b, c) in early stage (12- and 30-year) and topsoil belonged primarily to labile components with H/C $\geq$ 1.5 and O/C < 0.67 (Fig. 3), such as lipid- and protein-like compounds, indicating a higher accumulation of microbially-derived DOM (Li et al., 2019). In contrast, DOM chemo-markers in late stage (80- and 120-year) and subsoil were dominated by stable DOM with a wider O/C and H/C < 1.5, such as tannin- and condensed aromatic-like compounds (Fig. 3b, c) (Li et al., 2019; Hu et al., 2022). Tannins, one type of plant polyphenol, are toxic for most microbes (Wang et al., 2018), and are precipitate with lipids and proteins (Niu et al., 2022). Therefore, tannin-like compounds slowed down the production of microbially-derived DOM in the late stage (Fig. 3a). Moreover, saprophytic fungi can convert lignin to oxygenated tannins (humification of wood chips) (Khatami et al., 2019). Waggoner et al. (2015) proposed a non-pyrogenic formation of condensed aromatic compounds from lignin, which may explain why proportions of lignin-like compounds were lower, while tannin- and condensed aromatic-like compounds were abundant in the late stage (Fig. 3a). This suggests a transition from microbially-derived DOM production, primarily utilizing labile DOM, to plant-derived DOM decomposition, mainly utilizing stable DOM during initial pedogenesis.

As a young ecosystem, retreating glacier forefield is accompanied by vegetation succession and initial soil formation (He and Tang, 2008; Li et al., 2023). Vegetation succession in this deglaciated area has following patterns: i) mosses and pioneer N_2-fixing shrubs (*Astragalus adsurgens* and *Hippophae rhamnoides*) colonized during the 12- and 30-year retreat (early stage); ii) 40- and 52-year (middle stage) vegetation was dominated by *H. rhamnoides* and broadleaved trees such as *Salix* spp. and *Populus purdomii*; iii) coniferous *Abies fabri* and *Picea brachytyla* trees dominated at 80- and 120-year (late stage) (Lei et al., 2015; Lei et al., 2021; Jiang et al., 2018; Jiang et al., 2019). N_2-fixing plants possess more readily decomposable litterfall and root residues (Ye et al., 2020), which are preferentially consumed by microbes and transformed to microbially-derived DOM (Roth et al., 2019). This explains the increase of lipid- and protein-like compounds in the early stage and topsoil (Fig. 3). DOM in the late stage and subsoil was enriched with high-molecular-weight (Fig. 1a) and plant-derived DOM (Fig. 2d, e; Fig. 3b, c), which may be attribute to a lower quality of litter (C/N > 60) from coniferous trees (Lei et al., 2015).

4.2. Co-variation of DOM chemo-diversity and soil microbial communities

DOM interactions with microorganisms can be viewed through molecular ecological networks. Although glacier retreat and vegetation succession influence DOM chemo-diversity and microbial communities (Roberts et al., 2009; Hagedorn et al., 2015; Zhou et al., 2020), it is not clear whether and how it affects the co-occurrence of DOM and microbes. The stable and labile DOM-microbial MENs were dominated by negative and positive networks, respectively (Fig. 6). Based on the resource-consumer relationships of DOM-microbial MENs, positive interactions are classified as the production of new molecules via biosynthetic processes, whereas negative interactions indicate the decomposition of larger molecules to smaller molecules (Zhou et al., 2020; Hu et al., 2022). Persistent components, such as tannin- and condensed aromatic-like compounds were negatively correlated with oligotrophs and saprophytes (Fig. 6a–c). Possible mechanisms of tannin-like compounds increased DOM persistence are i) High-molecular-weight tannins reduce N availability by binding to organic N compounds (Adamczyk et al., 2011); ii) Extracellular enzymes binding by tannins strongly reduce the DOM consumption by microbes (Triebwasser et al., 2012); iii) Polyphenols lower the bacteria-derived labile DOM production (Adamczyk et al., 2017), while mycorrhizal and saprophytic fungi can slowly decompose stable tannin-protein complexes (Wurzburger and Hendrick, 2009).

The positive interactions of DOM-microbial MENs decreased (Fig. 5a) with succession age, whereas the negative interactions (Fig. 5a), modularity (Table S2), and microbial hubs (Fig. 5b) increased. The increased negative interactions further confirmed that microbially-decomposed DOM was enriched during the succession (Fig. 3). Due to the increasing negative associations, much more microbial hubs reflect highly diverse DOM decomposition from microbial communities (Zhou et al., 2020), whereas greater modularity indicates an increased stability (Chen et al., 2019; Hernandez et al., 2021; Li et al., 2022) of decomposition networks. The increase of microbially-decomposed DOM was also indicated by the raise of negative DOM-fungal edges and negative DOM-bacterial edges in topsoil (slope = 2.52, R^2 = 0.99) and subsoil (slope = 2.52, R^2 = 0.94), respectively (Fig. S2), causing the temporal and vertical differentiation of DOM metabolic niches for microbial utilization (Ye et al., 2020). More specifically, DOM decomposition in topsoil relied more strongly on fungi during the succession, whereas DOM decomposition in the subsoil was more dependent on bacteria. One explanation is that vegetation succession from shrubs to grassland and forest leads to more persistent organic compounds in topsoil, such as coniferous litterfall, which relies more strongly on fungi-mediated specialists to decomposition (Wei et al., 2020). Another possibility is that the intensive precipitation (approximately 2000 mm per year) accelerates the leaching of readily decomposable substrates from the topsoil to the subsoil, and the humid and mild climate is more favorable for a fast bacterial turnover during DOM downward transport (Lei et al., 2015).

4.3. Microbial assemblage links to DOM molecular transformation during initial soil formation

DOM interactions with microorganisms are affected by microbial life-history traits (Muscarella et al., 2019; Deng et al., 2020). To confirm the role of microbes in DOM molecular transformation, we constructed a co-occurrence network between microbial communities and the above-mentioned chemo-marker DOM. *Proteobacteria* and *Actinobacteriota* were negatively correlated with persistent DOM (such as lignin-, tannin-, and condensed aromatic-like compounds) in the early and middle stage, but were increased with persistent DOM content in late stage (Fig. 6a–c). This suggests *Proteobacteria* and *Actinobacteriota* mediate both decomposition and production of persistent DOM (St James et al., 2021). The hyphal morphology of *Actinobacteriota* can expand their C and nutrient acquisition from distant locations and are therefore, less specialized to the persistent DOM decomposition (Ling et al., 2022). In contrast, fungi (e.g. *Ascomycota* and *Mortierellomycota*) possessed more negative interactions with persistent DOM than bacteria (*Acidobacteria*) (Fig. 6c), indicating the dominance of fungal specialists to persistent DOM decomposition in the late stage. Notably, persistent DOM decomposition correlates with the

Fig. 5. Succession of soil DOM-microbial networks during chronosequence and depending on depth. (a) Co-occurrence network analysis for DOM molecular formulas and microbial communities. Nodes represent individual DOM molecular formulas and microbial phyla, with sizes that are positively correlated with the node degree. Edges represent significant Spearman correlations ($r > 0.9$ and $p < 0.001$); red lines indicate positive correlations and green lines indicate negative correlations. (b) The identification of network hubs (degree >25 with closeness centrality >0.2) in DOM-microbial MENs.

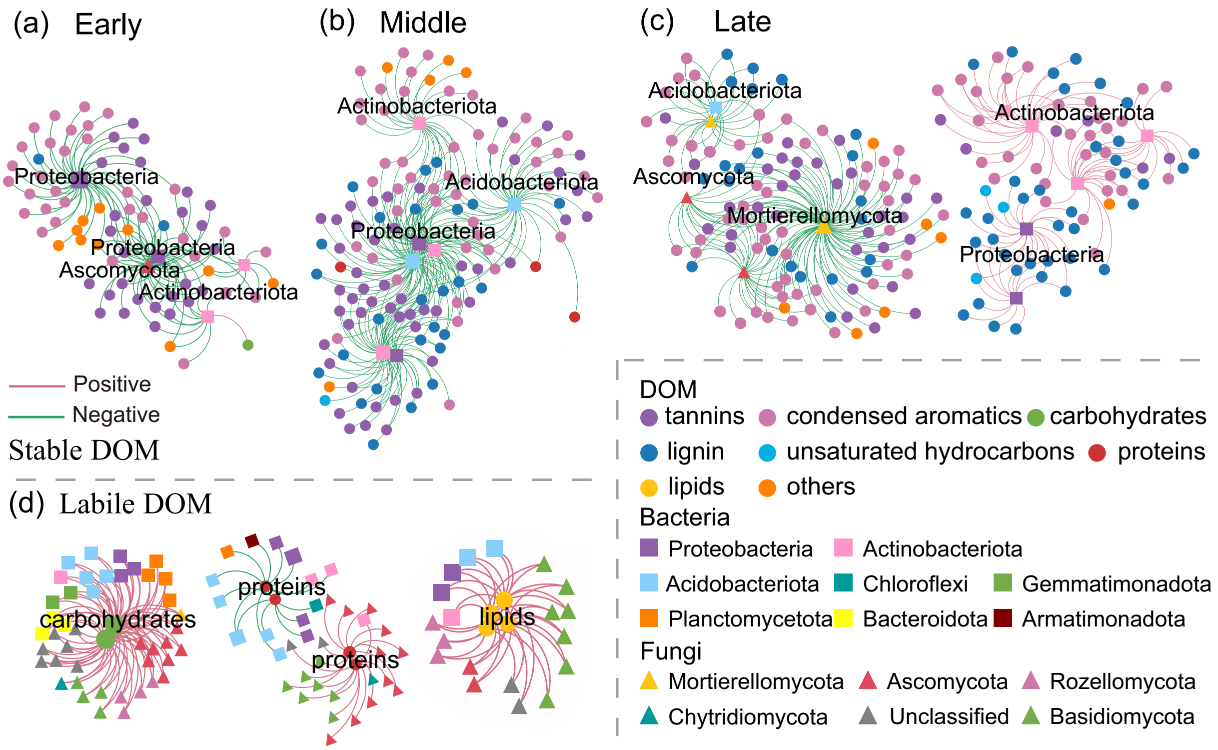

Fig. 6. Interactions of chemo-marker DOM compounds and microbial communities. Co-occurrence network analysis of stable DOM components ($H/C < 1.5$) and microbial communities in early (a), middle (b), and late stages (c), respectively. (d) Co-occurrence network analysis of labile DOM ($H/C \geq 1.5$) and microbial communities (All stages). Sizes of the nodes (circles) are proportioned to the number of connections (degree).

colonization and assembly of oligotrophs and saprophytes (Veach et al., 2019). Thus, a much higher abundance of *Acidobacteria* and *Mortierellomycota* in the late stage (Fig. 4a) suggested oligotrophs and saprophytes decompose slowly the stable DOM pools, indicating a greater DOM persistence. Although *Acidobacteria* members are *K*-selected oligotrophs that specialize to decompose stable DOM (Ling et al., 2022), *Acidobacteria* were dominant in utilization of both stable and labile substances (Fig. 6). These observations are consistent with Kielak et al. (2016) confirmed an affinity of *Acidobacteria* for both stable and easily degradable C sources.

4.4. Implications and uncertainties

Understanding the temporal and vertical dynamics of soil DOM composition, microbial communities, and their interaction networks after deglaciation, have profound impacts on evaluating the fate and persistence of soil DOM under future climate change. During post-glacial pedogenesis, there was a transition from bacteria-dominated positive networks, primarily utilizing labile DOM, to fungi-dominated negative networks, specially utilizing stable DOM. The dominance of oligotrophic and saprophytic fungi might be linked to the shift from microbial growth limitations from C and N to phosphorus (P) in the late pedogenesis (Jiang et al., 2018; Jiang et al., 2019), because P will be intensively leached at a mean annual precipitation of 2000 mm. Nevertheless, considering the contentious view of nutrient limitation during pedogenesis, revisiting and characterizing the edaphic and biotic drivers of DOM generalists vs. DOM specialists thus seem warranted.

Several uncertainties should be considered. The definition of low, mid, and high molecular weight DOM in the m/z range of 100–800 Da was introduced by Roth et al. (2019), which aims to filter the interference peaks from molecular weight lists (Patriarca and Hawkes, 2020). It is evident, however, that such distinguishability of low, mid, and high molecular weight through a narrow window captured by FT-ICR MS has limitations to its applicability. For instance, when ultrafiltration is used to separate DOM, all of them described here might fall into the category of low molecular weight DOM. Thus, improved ultrafiltration methods may allow exploration for more variable molecular weight DOM in the future. In co-occurrence network analysis, the relative method might increase the intragroup variability among molecular formulas as FT-ICR MS does not provide quantitative information on the molecular compounds. But actually, the variability of DOM-microbial co-occurrence was much greater than that among the molecular formulas (Li et al., 2019; Hu et al., 2022). Furthermore, additional studies have shown that over 20 % of soil total mobile organic carbon are particulate organic matter (POM, > 0.45 μm), which potentially contribute to pedogenesis, functioning, and nutritional supply of soil ecosystems (Lehmann et al., 2021). Further investigations are warranted to address microbial interactions into the DOM-POM continuum for a more comprehensive understanding of microbial metabolism, specialization, and contribution on soil total mobile inventory.

5. Conclusions

During a 120-year initial soil formation on the glacial forefield chronosequence, DOM were progressively dehydrogenated and oxidized, and transformed towards much lower H/C and higher molecular weight, double bond equivalent, and oxygen to carbon ratios. DOM in early stage (12 and 30 years) and middle stage (40 and 52 years), as well as in topsoil were enriched by labile compounds (lipid- and protein-like compounds with $H/C \geq 1.5$ and $O/C < 0.67$). DOM in late stage (80 and 120 years) and subsoil contained more persistent compounds (tannin- and condensed aromatic-like compounds with $H/C < 1.5$ and wider O/C). The succession directed microbial communities from eutrophic bacteria (*r* strategists) towards oligotrophic and saprophytic fungi (mainly *K* strategists). The modularity, microbial hubs, and negative connectivity of DOM-microbial networks increased with soil age and depth, which stimulate fungal specialists to decompose stable DOM. Consequently, DOM is not intrinsically persistent during post-

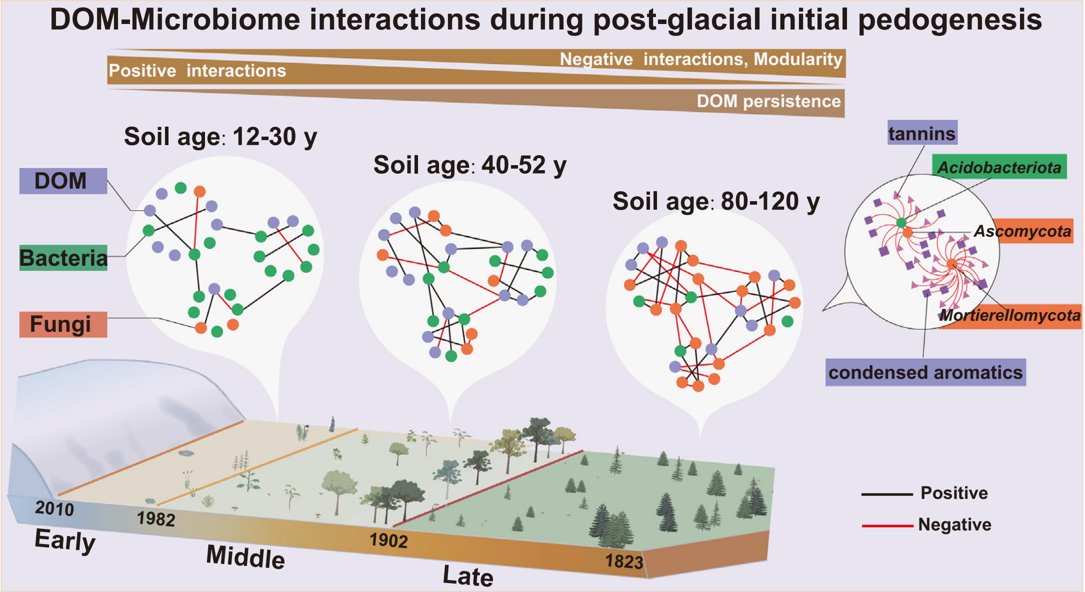

Fig. 7. Concept of interactions between DOM and microbial community composition and networks during post-glacial initial pedogenesis. Glacial retreat periods are accompanied by vegetation succession, soil development, and microbial community changes. Interactions between DOM and microbial networks are presented at the top.

glacial initial pedogenesis; rather, it persists in soil by decreased production of microbially-derived DOM (less bacteria-dominated positive networks) and increased decomposition of plant-derived DOM (more fungi-dominated negative networks) (Fig. 7).

CRediT authorship contribution statement

Jie Shen: Conceptualization, Investigation, Formal analysis, Data curation, Visualization, Writing-original draft. **Ziyan Liang:** Investigation, Data curation, Formal analysis, Visualization. **Yakov Kuzyakov:** Review & Editing. **Weitao Li:** Data curation, Visualization, Review & Editing. **Yuting He:** Language Editing & Methodology. **Changquan Wang:** Review & Editing. **Yang Xiao:** Formal analysis, Data curation & Visualization. **Ke Chen:** Review & Editing. **Geng Sun:** Methodology, Supervision, Review & Editing. **Yanbao Lei:** Conceptualization, Methodology, Funding acquisition, Supervision, Review & Editing.

Data availability

Data will be made available on request.

Declaration of competing interest

The authors declare that they have no known competing financial interests or personal relationships that could have influenced the work reported in this paper.

Acknowledgements

This study was jointly supported by the National Natural Science Foundation of China (31971632, 32241035), China Postdoctoral Science Foundation (2022M713071), the Second Tibetan Plateau Scientific Expedition and Research Program (2019QZKK0302-02), the National Key Research and Development Program of China (2020YFE0203200), Sichuan Science & Technology Bureau (2021YFH0008, 2022ZYD0122, 2022YFS0492, 2022YFH0040 and 2022JDGD0007), the Strategic Academic Leadership Program "Priority 2030" of the Kazan Federal University, the RUDN University Strategic Academic Leadership Program, and Jiuzhaigou Post-Disaster Restoration and Reconstruction Program. We gratefully appreciate Dr. Xiaoming Li from Research Center for Eco-Environmental Sciences, CAS for constructive comments, Majorbio, Inc. (Shanghai, China) for high-throughput sequencing service.

Appendix A. Supplementary data

Supplementary data to this article can be found online at https://doi.org/10.1016/j.scitotenv.2023.163171.

References

Adamczyk, B., Adamczyk, S., Smolander, A., Kitunen, V., 2011. Tannic acid and Norway spruce condensed tannins can precipitate various organic nitrogen compounds. Soil Biol. Biochem. 43, 628–637.

Adamczyk, B., Simon, J., Kitunen, V., Adamczyk, S., Smolander, A., 2017. Tannins and their complex interaction with different organic nitrogen compounds and enzymes: old paradigms versus recent advances. ChemistryOpen 6, 610–614.

Baker, K.L., Langenheder, S., Nicol, G.W., Ricketts, D., Killham, K., Campbell, C.D., Prosser, J.I., 2009. Environmental and spatial characterisation of bacterial community composition in soil to inform sampling strategies. Soil Biol. Biochem. 41, 2292–2298.

Blackburn, J.W.T., Kew, W., Graham, M.C., Uhrín, D., 2017. Laser desorption/ionization coupled to FTICR mass spectrometry for studies of natural organic matter. Anal. Chem. 89, 4382–4386.

Bradley, J.A., Arndt, S., Šabacká, M., Benning, L.G., Barker, G.L., Blacker, J.J., Yallop, M.L., Wright, K.E., Bellas, C.M., Telling, J., Tranter, M., Anesio, A.M., 2016. Microbial dynamics in a High Arctic glacier forefield: a combined field, laboratory, and modelling approach. Biogeosciences 13, 5677–5696.

Broadbent, A.A.D., Snell, H.S.K., Michas, A., Pritchard, W.J., Newbold, L., Cordero, I., Goodall, T., Schallhart, N., Kaufmann, R., Griffiths, R.I., Schloter, M., Bahn, M., Bardgett, R.D., 2021. Climate change alters temporal dynamics of alpine soil microbial functioning and biogeochemical cycling via earlier snowmelt. ISME J. 15, 2264–2275.

Castle, S.C., Sullivan, B.W., Knelman, J., Hood, E., Nemergut, D.R., Schmidt, S.K., Cleveland, C.C., 2017. Nutrient limitation of soil microbial activity during the earliest stages of ecosystem development. Oecologia 185, 513–524.

Chen, L., Xiang, W.H., Wu, H.L., Ouyang, S., Lei, P.F., Hu, Y.J., Ge, T.D., Ye, J., Kuzyakov, Y., 2019. Contrasting patterns and drivers of soil fungal communities in subtropical deciduous and evergreen broadleaved forests. Appl.Microbiol.Biotechnol. 103 (13), 5421–5433.

D'Andrilli, J., Cooper, W.T., Foreman, C.M., Marshall, A.G., 2015. An ultrahigh-resolution mass spectrometry index to estimate natural organic matter lability. Rapid Commun. Mass Spectrom. 29, 2385–2401.

Deng, S., Zheng, X., Chen, X., Zheng, S., He, X., Ge, T., Kuzyakov, Y., Wu, J., Su, Y., Hu, Y., 2020. Divergent mineralization of hydrophilic and hydrophobic organic substrates and their priming effect in soils depending on their preferential utilization by bacteria and fungi. Biol. Fertil. Soils 57, 65–76.

Fierer, N., Bradford, M.A., Jackson, R.B., 2007. Toward an ecological classification of soil bacteria. Ecology 88, 1354–1364.

Franklin, H.M., Carroll, A.R., Chen, C., Maxwell, P., Burford, M.A., 2020. Plant source and soil interact to determine characteristics of dissolved organic matter leached into waterways from riparian leaf litter. Sci. Total Environ. 703, 134530.

Gyeong, H., Hyun, C., Kim, S.C., Tripathi, B.M., Yun, J., Kim, J., Kang, H., Kim, J.H., Kim, S., Kim, M., 2021. Contrasting early successional dynamics of bacterial and fungal communities in recently deglaciated soils of the maritime Antarctic. Mol. Ecol. 30, 4231–4244.

Hagedorn, F., Bruderhofer, N., Ferrari, A., Niklaus, P.A., 2015. Tracking litter-derived dissolved organic matter along a soil chronosequence using 14C imaging: biodegradation, physico-chemical retention or preferential flow? Soil Biol. Biochem. 88, 333–343.

He, L., Tang, Y., 2008. Soil development along primary succession sequences on moraines of Hailuogou Glacier, Gongga Mountain, Sichuan, China. Catena 72, 259–269.

He, C., Jiang, B., Shi, Q., Hsu, C.S., 2018. Comment on “Laser desorption/ionization coupled to FTICR mass spectrometry for studies of natural organic matter”. Anal. Chem. 90, 5965–5967.

Hernandez, D.J., David, A.S., Menges, E.S., Searcy, C.A., Afkhami, M.E., 2021. Environmental stress destabilizes microbial networks. ISME J. 15, 1722–1734.

Hu, A., Choi, M., Tanentzap, A.J., Liu, J., Jang, K.S., Lennon, J.T., Liu, Y., Soininen, J., Lu, X., Zhang, Y., Shen, J., Wang, J., 2022. Ecological networks of dissolved organic matter and microorganisms under global change. Nat. Commun. 13, 3600.

Huang, H., Jia, Y., Sun, G.X., Zhu, Y.G., 2012. Arsenic speciation and volatilization from flooded paddy soils amended with different organic matters. Environ.Sci.Technol. 46, 2163–2168.

Jiang, Y.L., Lei, Y.B., Yang, Y., Korpelainen, H., Niinemets, Ü., Li, C.Y., 2018. Divergent assemblage patterns and driving forces for bacterial and fungal communities along a glacier forefield chronosequence. Soil Biol. Biochem. 118, 207–216.

Jiang, Y.L., Lei, Y.B., Qin, W., Korpelainen, H., Li, C.Y., 2019. Revealing microbial processes and nutrient limitation in soil through ecoenzymatic stoichiometry and glomalin-related soil proteins in a retreating glacier forefield. Geoderma 338, 313–324.

Kaiser, K., Kalbitz, K., 2012. Cycling downwards – dissolved organic matter in soils. Soil Biol. Biochem. 52, 29–32.

Kallenbach, C.M., Frey, S.D., Grandy, A.S., 2016. Direct evidence for microbial-derived soil organic matter formation and its ecophysiological controls. Nat. Commun. 7, 13630.

Khatami, S., Deng, Y., Tien, M., Hatcher, P.G., 2019. Formation of water-soluble organic matter through fungal degradation of lignin. Org. Geochem. 135, 64–70.

Kielak, A.M., Barreto, C.C., Kowalchuk, G.A., van Veen, J.A., Kuramae, E.E., 2016. The ecology of Acidobacteria: moving beyond genes and genomes. Front. Microbiol. 7, 744.

Koch, B.P., Dittmar, T., 2006. From mass to structure: an aromaticity index for high-resolution mass data of natural organic matter. Rapid Commun. Mass Spectrom. 20, 926–932.

Lehmann, K., Lehmann, R., Totsche, K.U., 2021. Event-driven dynamics of the total mobile inventory in undisturbed soil account for significant fluxes of particulate organic carbon. Sci. Total Environ. 756, 143774.

Lei, Y.B., Zhou, J., Xiao, H.F., Duan, B.L., Wu, Y.H., Korpelainen, H., Li, C.Y., 2015. Soil nematode assemblages as bioindicators of primary succession along a 120-year-old chronosequence on the Hailuogou Glacier forefield, SW China. Soil Biol. Biochem. 88, 362–371.

Lei, Y., Du, L.S., Chen, K., Plenković-Moraj, A., Sun, G., 2021. Optimizing foliar allocation of limiting nutrients and fast-slow economic strategies drive forest succession along a glacier retreating chronosequence in the eastern Tibetan Plateau. Plant Soil 462, 159–174.

Leinweber, P., Eckhardt, K.U., Fischer, H., Kuzyakov, Y., 2008. A new rapid micro-method for the molecular-chemical characterization of rhizodeposits by field-ionization mass spectrometry. Rapid Commun. Mass Spectrom. 22 (8), 1230–1234.

Li, H.Y., Wang, H., Wang, H.T., Xin, P.Y., Xu, X.H., Ma, Y., Liu, W.P., Teng, C.Y., Jiang, C.L., Lou, L.P., Arnold, W., Cralle, L., Zhu, Y.G., Chu, J.F., Gilbert, J., Zhang, Z.J., 2018. The chemodiversity of paddy soil dissolved organic matter correlates with microbial community at continental scales. Microbiome 6, 187.

Li, X.M., Sun, G.X., Chen, S.C., Fang, Z., Yuan, H.Y., Shi, Q., Zhu, Y.G., 2018. Molecular chemodiversity of dissolved organic matter in paddy soils. Environ. Sci. Technol. 52, 963–971.

Li, X.M., Chen, Q.L., He, C., Shi, Q., Chen, S.C., Reid, B.J., Zhu, Y.G., Sun, G.X., 2019. Organic carbon amendments affect the chemodiversity of soil dissolved organic matter and its associations with soil microbial communities. Environ.Sci.Technol. 53, 50–59.

Li, W.T., Kuzyakov, Y., Zheng, Y.L., Li, P.F., Li, G.L., Liu, M., Alharbi, H.A., Li, Z.P., 2022. Depth effects on bacterial community assembly processes in paddy soils. Soil Biol. Biochem. 165, 108517.

Li, W.T., Lu, Q., Alharbi, S.A., Soromotin, A.V., Kuzyakov, Y., Lei, Y.B., 2023. Plant–soil–microbial interactions mediate vegetation succession in retreating glacial forefields. Sci. Total Environ. 873, 162393.

Ling, L., Luo, Y., Jiang, B., Lv, J., Meng, C., Liao, Y., Reid, B.J., Ding, F., Lu, Z., Kuzyakov, Y., Xu, J., 2022. Biochar induces mineralization of soil recalcitrant components by activation of biochar responsive bacteria groups. Soil Biol. Biochem. 172, 108778.

Lucas, J., Koester, I., Wichels, A., Niggemann, J., Dittmar, T., Callies, U., Wiltshire, K.H., Gerdts, G., 2016. Short-term dynamics of north sea bacterioplankton-dissolved organic matter coherence on molecular level. Front. Microbiol. 7, 321.

Minor, E.C., Swenson, M.M., Mattson, B.M., Oyler, A.R., 2014. Structural characterization of dissolved organic matter: a review of current techniques for isolation and analysis. Environ.Sci.: Processes Impacts 16, 2064–2079.

Muscarella, M.E., Boot, C.M., Broeckling, C.D., Lennon, J.T., 2019. Resource heterogeneity structures aquatic bacterial communities. ISME J. 13, 2183–2195.

Mushinski, R.M., Zhou, Y., Gentry, T.J., Boutton, T.W., 2018. Bacterial metataxonomic profile and putative functional behavior associated with C and N cycle processes remain altered for decades after forest harvest. Soil Biol. Biochem. 119, 184–193.

Neilen, A.D., Carroll, A.R., Hawker, D.W., O'Brien, K.R., Burford, M.A., 2019. Effects of photochemical and microbiological changes in terrestrial dissolved organic matter on its chemical characteristics and phytotoxicity towards cyanobacteria. Sci. Total Environ. 695, 133901.

Niu, G., Yin, G., Mo, X., Mao, Q., Mo, J., Wang, J., Lu, X., 2022. Do long-term high nitrogen inputs change the composition of soil dissolved organic matter in a primary tropical forest? Environ. Res. Lett. 17, 095015.

Osterholz, H., Singer, G., Wemheuer, B., Daniel, R., Simon, M., Niggemann, J., Dittmar, T., 2016. Deciphering associations between dissolved organic molecules and bacterial communities in a pelagic marine system. ISME J. 10, 1717–1730.

Patriarca, C., Hawkes, J.A., 2020. High molecular weight spectral interferences in mass spectra of dissolved organic matter. J. Am. Soc. Mass Spectrom. 32, 394–397.

Peng, J., Wegner, C.E., Bei, Q., Liu, P., Liesack, W., 2018. Metatranscriptomics reveals a differential temperature effect on the structural and functional organization of the anaerobic food web in rice field soil. Microbiome 6, 169.

Roberts, P., Newsham, K.K., Bardgett, R.D., Farrar, J.F., Jones, D.L., 2009. Vegetation cover regulates the quantity, quality and temporal dynamics of dissolved organic carbon and nitrogen in Antarctic soils. Polar Biol. 32, 999–1008.

Roth, V.N., Lange, M., Simon, C., Hertkorn, N., Bucher, S., Goodall, T., Griffiths, R.I., Mellado-Vázquez, P.G., Mommer, L., Oram, N.J., Weigelt, A., Dittmar, T., Gleixner, G., 2019. Persistence of dissolved organic matter explained by molecular changes during its passage through soil. Nat. Geosci. 12, 755–761.

Saidy, A.R., Smernik, R.J., Baldock, J.A., Kaiser, K., Sanderman, J., 2013. The sorption of organic carbon onto differing clay minerals in the presence and absence of hydrous iron oxide. Geoderma 209–210, 15–21.

Sanderman, J., Baldock, J.A., Amundson, R., 2008. Dissolved organic carbon chemistry and dynamics in contrasting forest and grassland soils. Biogeochemistry 89, 181–198.

Šantl-Temkiv, T., Finster, K., Dittmar, T., Hansen, B.M., Thyrhaug, R., Nielsen, N.W., Karlson, U.G., 2013. Hailstones: a window into the microbial and chemical inventory of a storm cloud. PloS One 8, e53550.

Segata, N., Izard, J., Waldron, L., Gevers, D., Miropolsky, L., Garrett, W.S., Huttenhower, C., 2011. Metagenomic biomarker discovery and explanation. Genome Biol. 12, R60.

Shen, J., Luo, Y., Tao, Q., White, P.J., Sun, G., Li, M., Luo, J., He, Y., Li, B., Li, Q., Xu, Q., Cai, Y., Li, H., Wang, C., 2022. The exacerbation of soil acidification correlates with structural and functional succession of the soil microbiome upon agricultural intensification. Sci. Total Environ. 828, 154524.

Shipley, B., Tardif, A., 2020. Causal hypotheses accounting for correlations between decomposition rates of different mass fractions of leaf litter. Ecology 102, 1–9.

St James, A.R., Yavitt, J.B., Zinder, S.H., Richardson, R.E., 2021. Linking microbial Sphagnum degradation and acetate mineralization in acidic peat bogs: from global insights to a genome-centric case study. ISME J. 15, 293–303.

Tanentzap, A., Fitch, A., Orland, C., Emilson, E., Yakimovich, K., Osterholz, H., Dittmar, T., 2019. Chemical and microbial diversity covary in fresh water to influence ecosystem functioning. Proc. Natl. Acad. Sci. U. S. A. 116 (49), 24689–24695.

Tian, J., Fan, M.S., Guo, J.H., Marschner, P., Li, X.L., Kuzyakov, Y., 2012. Effects of land use intensity on dissolved organic carbon properties and microbial community structure. Eur. J. Soil Biol. 52, 67–72.

Triebwasser, D.J., Tharayil, N., Preston, C.M., Gerard, P.D., 2012. The susceptibility of soil enzymes to inhibition by leaf litter tannins is dependent on the tannin chemistry, enzyme class and vegetation history. New Phytol. 196, 1122–1132.

Veach, A.M., Morris, R., Yip, D.Z., Yang, Z.K., Engle, N.L., Cregger, M.A., Tschaplinski, T.J., Schadt, C.W., 2019. Rhizosphere microbiomes diverge among Populus trichocarpa plant-host genotypes and chemotypes, but it depends on soil origin. Microbiome 7, 76.

Vujinović, T., Zanin, L., Venuti, S., Contin, M., Ceccon, P., Tomasi, N., Pinton, R., Cesco, S., De Nobili, M., 2020. Biostimulant action of dissolved humic substances from a conventionally and an organically managed soil on nitrate acquisition in maize plants. Front. Plant Sci. 10, 1652.

Waggoner, D.C., Chen, H., Willoughby, A.S., Hatcher, P.G., 2015. Formation of black carbon-like and alicyclic aliphatic compounds by hydroxyl radical initiated degradation of lignin. Org. Geochem. 82, 69–76.

Wang, X., Wang, J., Zhang, Y., Shi, Q., Zhang, H., Zhang, Y., Yang, M., 2016. Characterization of unknown iodinated disinfection byproducts during chlorination/chloramination using ultrahigh resolution mass spectrometry. Sci. Total Environ. 554–555, 83–88.

Wang, C., Lu, X., Mori, T., Mao, Q., Zhou, K., Zhou, G., Nie, Y., Mo, J., 2018. Responses of soil microbial community to continuous experimental nitrogen additions for 13 years in a nitrogen-rich tropical forest. Soil Biol. Biochem. 121, 103–112.

Wang, L., Zhou, Y., Chen, Y., Xu, Z., Zhang, J., Liu, Y., Joly, F.X., 2022. Litter diversity accelerates labile carbon but slows recalcitrant carbon decomposition. Soil Biol. Biochem. 168, 108632.

Wei, X., Yang, Y., Shen, Y., Chen, Z., Dong, Y., Wu, F., Zhang, L., 2020. Effects of litterfall on the accumulation of extracted soil humic substances in subalpine forests. Front. Plant Sci. 11, 254.

Wei, Y., Xiong, X., Ryo, M., Badgery, W.B., Bi, Y., Yang, G., Zhang, Y., Liu, N., 2022. Repeated litter inputs promoted stable soil organic carbon formation by increasing fungal dominance and carbon use efficiency. Biol. Fertil. Soils 58, 619–631.

Wen, T., Yu, G.H., Hong, W.D., Yuan, J., Niu, G.Q., Xie, P.H., Sun, F.S., Guo, L.D., Kuzyakov, Y., Shen, Q.R., 2022. Root exudate chemistry affects soil carbon mobilization via microbial community reassembly. Fundam.Res. 2, 697–707.

Wu, X., Wu, L., Liu, Y., Zhang, P., Li, Q., Zhou, J., Hess, N.J., Hazen, T.C., Yang, W., Chakraborty, R., 2018. Microbial interactions with dissolved organic matter drive carbon dynamics and community succession. Front. Microbiol. 9, 1234.

Wu, M., Li, P., Li, G., Petropoulos, E., Feng, Y., Li, Z., 2021. The chemodiversity of paddy soil dissolved organic matter is shaped and homogenized by bacterial communities that are orchestrated by geographic distance and fertilizations. Soil Biol. Biochem. 161, 108374.

Wurzburger, N., Hendrick, R.L., 2009. Plant litter chemistry and mycorrhizal roots promote a nitrogen feedback in a temperate forest. J. Ecol. 97 (3), 528–536.

Ye, Q., Wang, Y.H., Zhang, Z.T., Huang, W.L., Li, L.P., Li, J., Liu, J., Zheng, Y., Mo, J.M., Zhang, W., Wang, J.J., 2020. Dissolved organic matter characteristics in soils of tropical legume and non-legume tree plantations. Soil Biol. Biochem. 148, 107880.

Zark, M., Dittmar, T., 2018. Universal molecular structures in natural dissolved organic matter. Nat. Commun. 9, 3178.

Zark, M., Christoffers, J., Dittmar, T., 2017. Molecular properties of deep-sea dissolved organic matter are predictable by the central limit theorem: evidence from tandem FT-ICR-MS. Mar. Chem. 191, 9–15.

Zeng, Z., Zheng, P., Ding, A., Zhang, M., Abbas, G., Li, W., 2017. Source analysis of organic matter in swine wastewater after anaerobic digestion with EEM-PARAFAC. Environ. Sci. Pollut. Res. 24, 6770–6778.

Zhang, C., Dang, H., Azam, F., Benner, R., Legendre, L., Passow, U., Polimene, L., Robinson, C., Suttle, C.A., Jiao, N., 2018. Evolving paradigms in biological carbon cycling in the ocean. Natl. Sci. Rev. 5, 481–499.

Zhou, J., Wu, Y., Prietzel, J., Bing, H., Yu, D., Sun, S., Luo, J., Sun, H., 2013. Changes of soil phosphorus speciation along a 120-year soil chronosequence in the Hailuogou Glacier retreat area (Gongga Mountain, SW China). Geoderma 195–196, 251–259.

Zhou, J., Bing, H., Wu, Y., Sun, H., Wang, J., 2018. Weathering of primary mineral phosphate in the early stages of ecosystem development in the Hailuogou Glacier foreland chronosequence. Eur. J. Soil Sci. 69, 450–461.

Zhou, J., Wu, Y., Turner, B., Sun, H., Wang, J., Bing, H., Luo, J., He, X., Zhu, H., He, Q., 2019. Transformation of soil organic phosphorus along the Hailuogou post-glacial chronosequence, southeastern edge of the Tibetan Plateau. Geoderma 352, 414–421.

Zhou, L., Zhou, Y., Yao, X., Cai, J., Liu, X., Tang, X., Zhang, Y., Jang, K.S., Jeppesen, E., 2020. Decreasing diversity of rare bacterial subcommunities relates to dissolved organic matter along permafrost thawing gradients. Environ. Int. 134, 105330.